Eur. Phys. J. Plus (2012) **127**: 126
DOI 10.1140/epjp/i2012-12126-7

THE EUROPEAN PHYSICAL JOURNAL PLUS

Regular Article

Malargüe seismic array: Design and deployment of the temporary array

E. Ruigrok[1,a], D. Draganov[1], M. Gómez[2], J. Ruzzante[2], D. Torres[2], I. Lópes Pumarega[2], N. Barbero[3], A. Ramires[3], A.R. Castaño Gañan[3], K. van Wijk[4], and K. Wapenaar[1]

[1] Department of Geoscience and Engineering, Delft University of Technology, Netherlands
[2] ICES, CNEA, Buenos Aires, Argentina
[3] ICES, CNEA, Malargüe, Argentina
[4] Boise State University, Physical Acoustics Laboratory, Department of Geosciences, Boise, Idaho, USA

Received: 13 September 2012
Published online: 17 October 2012 –

Abstract. We present the goals and the current status of the Malargüe seismic array. Our main goal is imaging and monitoring the subsurface below the Malargüe region, Mendoza, Argentina. More specifically, we focus on the Planchon-Peteroa Volcano and an area just east of the town of Malargüe. We start our project installing a temporary array of 38 seismic stations, which records continuously for one year. The array consists of two subarrays: one array located on the flanks of the volcano; the other spread out on a plateau just east of the Andes. The imaging targets, like the Moho and the Nazca slab, are relatively deep. Yet, the array has a dense station spacing, allowing exploration-type processing. For high-resolution imaging, also a dense source spacing is required. This we aim to achieve by creating virtual sources at the receiver positions, with a technique called seismic interferometry (SI). The array is designed such that a recent improvement of SI can be applied to the recordings. Other goals are to collect high-quality core-phase measurements and to characterize sources of microseism noise in the Southern Hemisphere. Furthermore, we plan to collaborate with researchers from the Pierre Auger Collaboration to study coupling of seismic, atmospheric, and cosmic signals using data from our instruments and from the Pierre Auger detectors.

1 Introduction

Seismology is the study of the vibration of the Earth. Seismologists pay much attention to the main source of Earth vibration: earthquakes, but also other seismic sources, like mining blasts, ocean storms and windmills, are studied. All these sources induce seismic waves, which can eventually be recorded as ground vibrations. These seismic records contain not only information about the source, but also about the medium through which the waves have propagated. A main subclass of seismology is seismic imaging, in which field seismic vibrations are studied with the aim to unravel the composition of the Earth.

Seismic imaging finds its main use in extracting information about the solid Earth that is within our reach. The deepest borehole (Kola, Russia) has only reached the upper 0.2 percent ($\approx 12\,\mathrm{km}$) of the Earth's radius. Only the upper 0.1 percent, however, is being mined. For this reachable range, seismic imaging can be used to find water reservoirs, hydrocarbon accumulations, karst holes, etc. This imaging, which aims at finding these substances and objects, is called exploration geophysics. Imaging the deep (*i.e.*, unreachable) Earth finds its main use in hazard assessment. Through imaging the deep Earth, we can better understand the dynamics of our planet, manifested in, amongst others, earthquakes and volcanism. Seismic characterization of the subsurface also improves our ability to assess the direct impact of earthquakes.

In the austral summer of 2012, during the months of January, March and April, we installed a large temporary seismic array in the Malargüe region, Mendoza, Argentina. This array is employed until the end of 2012. In the future, we plan to replace it by a permanent array. In the following section, the research goals of the seismic array are outlined as well as the choice for the Malargüe region. Section 3 highlights the design considerations for the temporary array.

[a] e-mail: E.N.Ruigrok@tudelft.nl

Further information about its deployment and the first data examples are given in sect. 4. In the end, in sect. 5, we discuss future plans.

2 Purpose of the array

2.1 Teaming up of Solid Earth and exploration geophysics

Traditionally, imaging of the deep Earth is performed using a sparse receiver network, covering a large part of the globe. Exploration geophysics, on the other hand, makes use of well-sampled receiver grids, covering only a specific target region. Deep-Earth imaging is primarily achieved with the use of natural sources (earthquakes), while, for exploration-scale imaging, well-sampled grids of controlled seismic sources, like dynamite and seismic vibrators, are used. The above differences between the two imaging methods led to the development of largely different imaging techniques. Unsurprisingly, the highest-resolution pictures of the Earth are made when many controlled sources and receivers are used. The technique developed to do this is called seismic reflection imaging (SRI; see, *e.g.*, [1]). To reach the deeper targets in the Earth using controlled sources, the latter should be quite powerful. This limits severely their utilization and in many areas even precludes it. Energetic natural sources, like large earthquakes, do illuminate the deep Earth.

During the last decade, exploration-type algorithms are increasingly finding their way to the deep-Earth community. One reason is that the cost of broad-band seismic stations, which are mostly employed for deep-Earth imaging, has come down. Moreover, a program has been set up to efficiently facilitate temporary deployments of broadband stations: Program for Array Seismic Studies of the Continental Lithosphere (PASSCAL), which is run by the Incorporated Research Institutions for Seismology (IRIS). Consequently, it has become feasible to deploy regional arrays to study portions of the deep Earth.

Beside the amount of receivers, also the amount of sources is effectively increasing. It is not that more earthquakes are occurring than in the past, but that a technique has been developed to create so-called virtual sources. This technique is called seismic interferometry (SI) [2–5]. SI can be looked at as a filtering operation. By the application of SI to the records at two seismic stations, the waves that hit upon the first station and then (multiply) reflect at subsurface interfaces before reaching the second station, are passed, while all other waves are suppressed. Consequently, a response can be obtained as if there were a virtual source at the first station and a receiver at the other. When SI is applied to a regularly spaced array of receivers, uncontrolled natural sources can be turned into a well-organized succession of virtual sources [6,7]. With a well-sampled array of virtual sources and receivers now available, SRI can be applied, and a detailed reflectivity image of the Earth's crust can be obtained [8–10].

A velocity model of the crust can be estimated with surface-wave tomography: inverting surface-wave velocity dispersion data [11]. Traditionally, surface-wave tomography is done with earthquake records. Due to the limited spatial distribution of earthquakes, the resolution of these velocity models was limited. However, besides earthquake-induced, a significant part of the Earth vibrations are related to interacting swell waves in the oceans. These interactions happen continuously and thus lead to the registration of noisy arrivals —the so-called microseisms [12]. By applying SI, these noisy registrations can be turned into a transient signal between two station positions. The retrieved surface waves can be used to improve the resolution of velocity models [13,14].

As described above, there is an increase in deployed regional arrays in seismology. However, most of these arrays are designed to apply single-station methods, like the receiver function [15], and lack a sufficiently dense sampling to allow exploration-type processing. Moreover, a technique has recently been developed to improve results from SI. For example, an irregular distribution of actual sources can lead to inaccuracies of the illumination pattern emitted by the retrieved virtual source. Given that the incoming wave fields are properly sampled, these inaccuracies can be corrected for. The technique to do this is called SI by multidimensional deconvolution (MDD) [16,17]. Thus, it was our aim to build an array with a dense-enough sampling to allow SI by MDD, followed by SRI.

2.2 Array location

There are a lot of interesting places on Earth to deploy a seismic array. Why locating one in the southern part of South America? Beside structural imaging, seismic arrays can be used to image seismic sources. It is our aim to better understand microseism sources in the Southern Pacific. Using well-sampled arrays of seismic stations allows us to find the directionality and elevation angle of the dominating noise sources, through, *e.g.*, beamforming [18]. By simultaneously beamforming at several arrays, the microseism-source areas can be triangulated with high resolution. In the Southern Hemisphere, however, there is a lack of seismic arrays, which limits the study of microseism sources [19]. To overcome this restriction, installation of a well-sampled array in the southern part of South America is necessary.

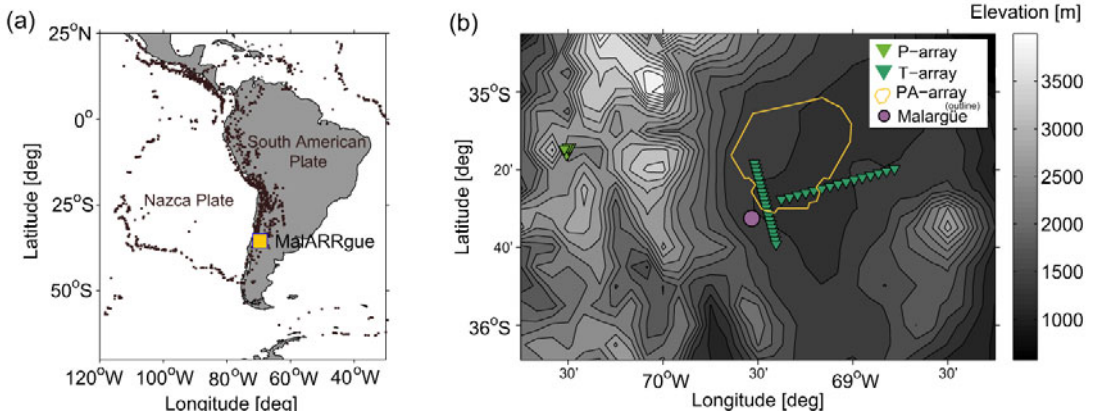

Fig. 1. (a) The tectonic setting of the Malargüe array. The black squares denote the epicenters of earthquakes with magnitude exceeding 5.0 (1997–2007). (b) Spatial distribution of the stations (green triangles) of the Malargüe array in their topographic setting (shades of grey). The array consists of two subarrays: the P-array (the light-green triangles; around 70°30′W longitude and 35°18′S latitude) and the T-array (dark-green triangles). The yellow line encompasses the region where Pierre Auger (PA) particle-detection stations are situated. In purple, the town of Malargüe is indicated.

Another purpose for choosing the southern part of South America is that the array can be used to detect and enhance the signal-to-noise ratio of arrivals from distant earthquakes. In particular, the array can be used to fill the gap in the database of high-quality core-phase measurements in the Southern Hemisphere.

Why locating the array in the Malargüe region? This region is situated between longitudes 68.25°W and 70.50°W and latitudes 34.75°S and 37.50°S, above the Nazca subduction zone (fig. 1a). It is about 250 km east of the Maule Region in Chile, where the devastating 2010 Chile earthquake occurred. This proximity and the active volcano in the Malargüe region (the Planchon-Peteroa Volcano, see sect. 3.1) are of constant concern for the local and regional population. The array could play an important role in hazard assessment, through characterization of the subsurface. In general, the subsurface of the southern part of South America is under-characterized. There have been several seismic studies in the past (*e.g.*, CHARGE, PUNA, PLUTONS), but nearly all of them have been to the north of the Malargüe region. Furthermore, these studies have been performed with a station spacing that precludes their utilization for detailed imaging of the underlying geology and detailed understanding of the volcanism in the region. Below the Malargüe region, the Moho (*i.e.*, the boundary between the Earth's crust and mantle) is significantly deeper than the world average of about 40 km. The topography of the nearby Andes has pushed it down to around 60 km. The depth to the Nazca slab has not been conclusively shown, but is believed to be around 170 km. Given the abundant volcanism in the area, the lithosphere must contain a number of magma intrusions, which have also not been imaged in any detail.

To assure that meaningful reflection responses are obtained after applying seismic interferometry, it is necessary to record ambient seismic noise containing identifiable body-wave arrivals. Normally, the body-wave noise is weaker than the surface-wave noise and this can preclude the implementation of SI for retrieval of reflection arrivals, which reflections are needed for SRI. The sources of surface-wave noise are natural, like the microseisms, and anthropogenic, like car traffic and heavy industry. Malargüe is situated at a high plateau directly east of the Andes. The Andes is partly shielding the surface-wave microseisms, which are induced at the Chilean coast and hence the array is expected to have good susceptibility for body waves induced on the pelagic Pacific. Furthermore, because of the low population density and little industrial activity, there is little disturbing anthropogenic seismicity near Malargüe.

Another reason for choosing the Malargüe region is the established connection with the international research community. In recent years, the region has seen the implementation and utilization of three permanent research installations: the southern part of the Pierre Auger (PA) observatory, a ground station from the worldwide space-tracking stations from the European Space Agency, and the acoustic-emission monitoring station from the International Center for Earth Sciences (ICES). The presence of these projects has two important advantages. The first is that the local authorities are predisposed to collaborate with the national and international scientific community and to help for the installation of a new scientific field laboratory. In addition, the local population and landowners are accustomed to the scientific work, accept it, and collaborate with what they can to facilitate it, as they have already seen the merits that it can bring to the local community. The third advantage is that local infrastructures and facilities, that make the installation of the seismic array easier, are already available. Furthermore, at least part of the array is closely located to the PA field stations and is intended to lead to collaboration with the PA project (sect. 5).

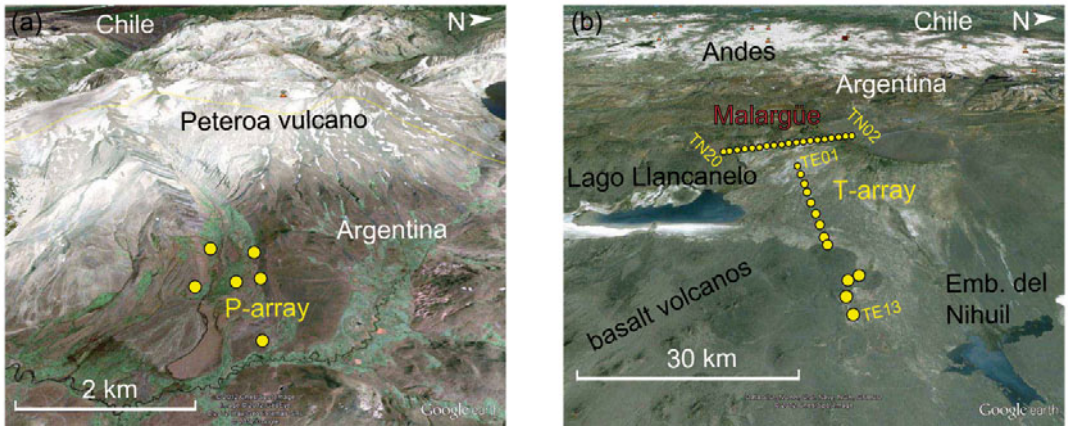

Fig. 2. The layout of the (a) P-array and (b) T-array on perspective-view satellite images of (a) the eastern flank of the Peteroa Volcano and (b) the Malargüe region. The yellow circles depict seismic stations.

3 Array design

The temporary array was designed as a multi-purpose antenna. The different purposes of the array can be categorized as 1) testing new structural-imaging algorithms, 2) source imaging and 3) hazard assessment. Using only 38 stations, aiming at achieving these different goals, means finding a compromise. Further design criteria included the terrain accessibility and permitting possibilities. Figure 2 shows the final geometry of the installed seismic stations. The array consists of two subarrays, the Peteroa array (P-array) and an array near the town of Malargüe that resembles a tilted letter T (the T-array). In the following, these two subarrays are described.

3.1 P-array

One large concern for the population of the Malargüe region is the Peteroa Volcano. There is fear of a repetition of the 1932 disaster when several centimeters of volcanic ashes from the eruption of the Descabezado Volcano to the south of the Malargüe region covered Malargüe. Since the late 1990s, Peteroa has reactivated. Its latest activity was in 2010, when it released fumes. Following the event, ICES installed a webcam at the base of the volcano, about 2500 m above sea level. The camera is part of a multiparametric measurement system. Another part of this system is a sensor station that registers the acoustic emission at the foot of the volcano. The recorded acoustic emissions are used to study the volcanic activity [20]. At the source of the thermal waters escaping from the volcano, ICES monitors the water temperature, the pH and the thermal conductivity of the water. Furthermore, ICES monitors the concentration of CO_2, gas typically related to volcanic activity, and the visible-light incidence in the zone. In 2012 also a Radon-meter will be installed.

The ICES measurements aim mainly at monitoring the surface activity of the volcano. The P-array will be used to image the structures under the surface and to monitor the activity at depth.

The temporary P-array consists of six stations located on the Eastern flank of the volcano (fig. 2a). The main goal of the array is to locate seismic activity related to magma flow below the crater. Conventionally, location of seismicity is done through backprojecting time differences of direct-wave arrivals. However, the data will also be used to test methods that use the multiply scattered wavefield.

Another technique that will be used to monitor the volcano is coda wave interferometry [21] using —when present— repeated volcanic sources [22] and using ambient noise [23]. The coda waves are the multiply scattered waves that arrive later in the seismic records. It is these waves that are most sensitive to minute changes in the medium. With coda wave interferometry, seismograms recorded (or retrieved with SI) at different times are compared. In this process, small time shifts of the coda waves are extracted and are related to medium changes below the volcano.

Besides the monitoring of seismic activity, the array's other goal is to image the structure of part of the volcano. This will be done using SI. We are planning to apply SI to ambient seismic noise. One path to follow is to retrieve surface-wave arrivals between the stations from SI and successively apply surface-wave tomography (*e.g.*, [24,25]). The velocity model obtained in such a way would allow for interpretation of the subsurface structures. We will also use SI for retrieval of reflection arrivals. For this, we will make use of autocorrelation (*e.g.*, [26]) of that part of the noise that contains body-wave arrivals. The obtained reflectivity information will be used in conjunction with the inverted velocity distributions from the dispersion curves to obtain better interpretation of the subsurface structures.

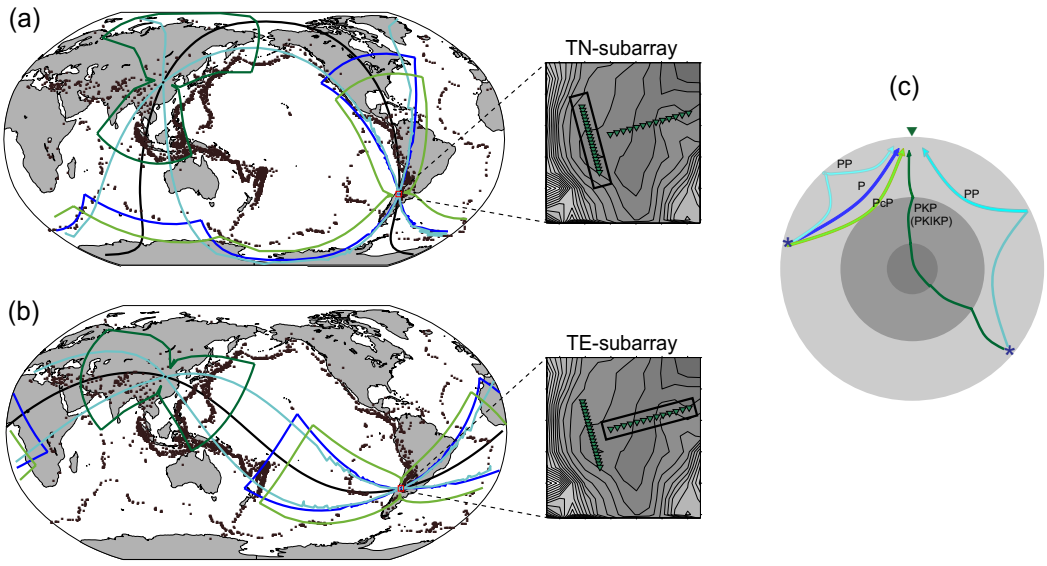

Fig. 3. Inline array illumination (for structural imaging), for (a) the TN-subarray and (b) the TE-subarray. On the left-hand side, world seismicity (brown squares) maps are shown. The black lines are a continuation of the great-circle paths connecting the different stations in the subarrays. The colored lines encompass source Fresnel zones [10] for which different types of arrivals (different colors), as defined in (c), could contribute to the retrieval of (multi-offset) reflections below the subarrays. On the right-hand side, the distribution of stations (green triangles) of the different subarrays is highlighted with a black box. *E.g.*, from (b) it can be seen that the P-phase from an earthquake near the Tonga Trench (north of New Zealand) would contribute to the retrieval of reflections below the TE-subarray.

Our stations cover only a limited part of the Peteroa Volcano (fig. 2a). The imaging and monitoring aperture will be extended through data exchange with the Observatorio Volcanológico de los Andes del Sur, which runs a seismic network at the Chilean site of the volcano.

3.2 T-array

The T-array is situated on a high plateau just east of the Andes (fig. 2b). The plateau is dotted by small volcano cones and lava flows. Besides, the surface is shaped by a large influx of melt water and sediments from the Andes.

The T-array consists of two subarrays, the TN-subarray, aligned in the NNW-SSE direction (fig. 3a), and the TE-subarray, aligned in the WSW-ENE direction (fig. 3b). A large part of the southern-hemisphere microseisms is induced at the Southern Pacific Ocean [27]. The array has been designed such that a large part of the microseism surface waves are captured by the TN-subarray prior to arriving at the TE-subarray. The TN array has a dense sampling of stations (one station every 2 km) to allow array processing with the incoming wave fields from the west. The station spacing is chosen such that the Nyquist spatial-sampling criterion is satisfied for the waves of interest. Consequently, SI by MDD can be implemented [17]. The result of the SI by MDD will be retrieved surface-wave arrivals between the different stations. These arrivals are then used to obtain dispersion curves which are inverted to obtain the velocity distributions at depth. The stations in the TE array are not used for array processing of (slow) surface-wave arrivals. Consequently, a larger average spacing of 4 km could be chosen and there was more flexibility to deviate from a straight line (fig. 2). The elevation differences within the TN and TE subarray are less than 75 m. Whether a static correction is required depends on the techniques and frequency bands used and the differences in near-surface conditions. The latter are for the moment largely unknown.

The TN-subarray is also aligned with the Andes orogeny and, in fact, with a large part of the Ring of Fire (fig. 3a). Thus, there are many earthquakes approximately inline with this subarray. Arrivals from these earthquakes can be used for reflectivity imaging below the array [8,10,28]. The TE-subarray captures sufficient global seismicity to allow deep-Earth imaging right below the array [29]. Furthermore, inline with the array there is microseism activity that could also be used for reflectivity imaging if a sufficient portion of body waves is induced.

The two subarrays will also be used together for retrieval of reflections using SI with ambient seismic noise [9,7]. For this, the surface-wave arrivals in the recorded noise should be suppressed and the body-wave arrivals enhanced. One way of achieving this is by selecting for retrieval only those parts of the noise that are dominated by body-wave arrivals, see [30].

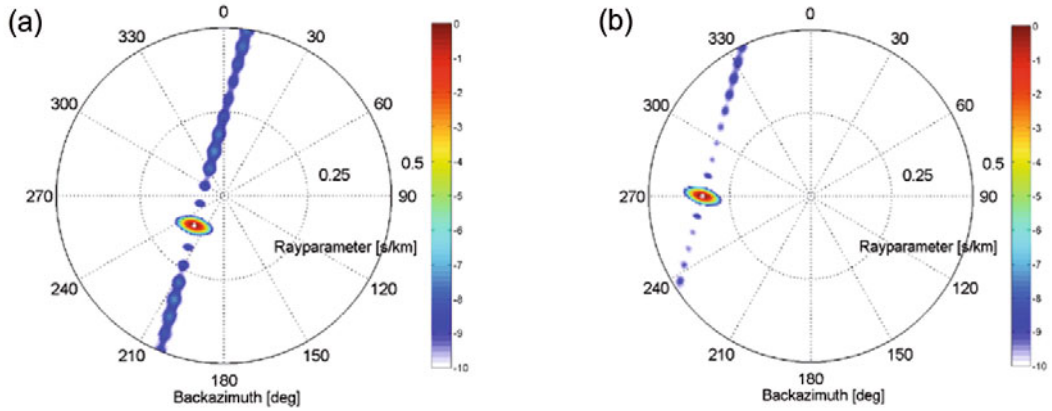

Fig. 4. Plane wave array response for the T-array, when (a) a 0.3 Hz body wave reaches it from the southwest with an apparent slowness of 0.125 s/km and (b) a 0.3 Hz surface wave reaches it from the west with an apparent slowness of 0.33 s/km.

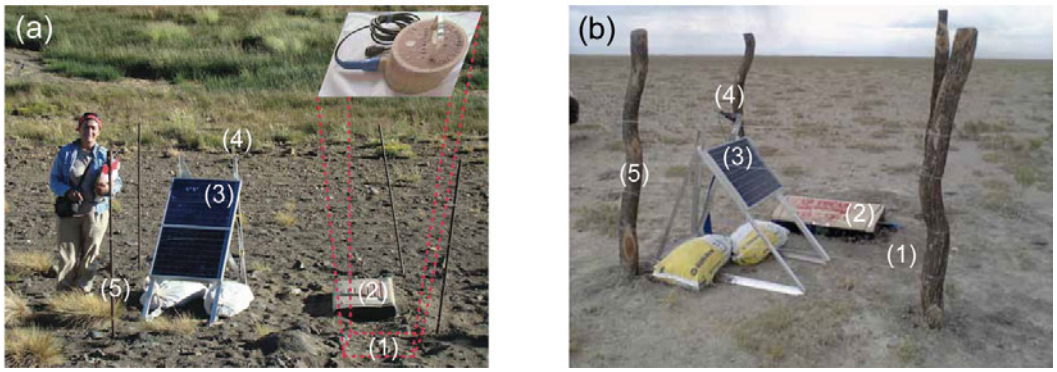

Fig. 5. Two seismic stations, (a) one from the P-array and (b) one from the T-array. The basic elements of each seismic station are (1) a buried seismometer (which is shown in the inset in (a)), (2) an equipment box with a datalogger, batteries and power box in it, (3) a solar panel, (4) a GPS clock and (5) a fence.

Besides for structural imaging, the T-array will be used to detect and locate seismic sources. The large number of stations —32— and the orthogonal configuration of the two subarrays allows an accurate estimation of backazimuth and elevation angle of incoming wave fields due to distant seismicity (fig. 4). For local and regional seismicity, additionally the curvature of the wave front is used to accurately estimate the source's spatial origin.

In the Malargüe Department there is another seismic network: Bloque San Rafael (BSR), which is run by the Universidad Nacional de San Juan. BSR is a sparse network, with a station spacing of approximately 40 km, covering a larger area than the T-array. It extends into the San Rafael Department, which is northeast of the Malargüe Department. Consequently, BSR compliments the T-array, and vice versa. Data exchange between the two networks would further improve the location of seismicity and allow high-resolution surface-wave tomography for the southern part of the Mendoza Province.

4 Array deployment

The seismic stations from the temporary array were installed in two field campaigns in January and in March-April 2012. Since then, the stations continuously record ambient seismic noise and earthquake activity. The recordings are stored locally at each station. The data from the T-array will be downloaded roughly every three months. Due to the difficulty in accessing the stations of the P-array in the winter, the data from the P-array will be downloaded after the snow in the mountains melts.

The P-array was installed in January. Figure 5(a) shows an example of an installed seismic station. It consists of a 2-Hz 3-component seismic sensor (Sercel L-22, see the inset in the figure), which is buried in the ground. The sensor is connected through a cable to a seismic recorder (Reftek 130B), which is placed inside the box (with a sand-color cover in fig. 5). Inside the box is also a battery for the solar panel, the latter is used to supply the needed electrical power for the functioning of the equipment. The station is also equipped with a GPS clock for exact timing of recorded events.

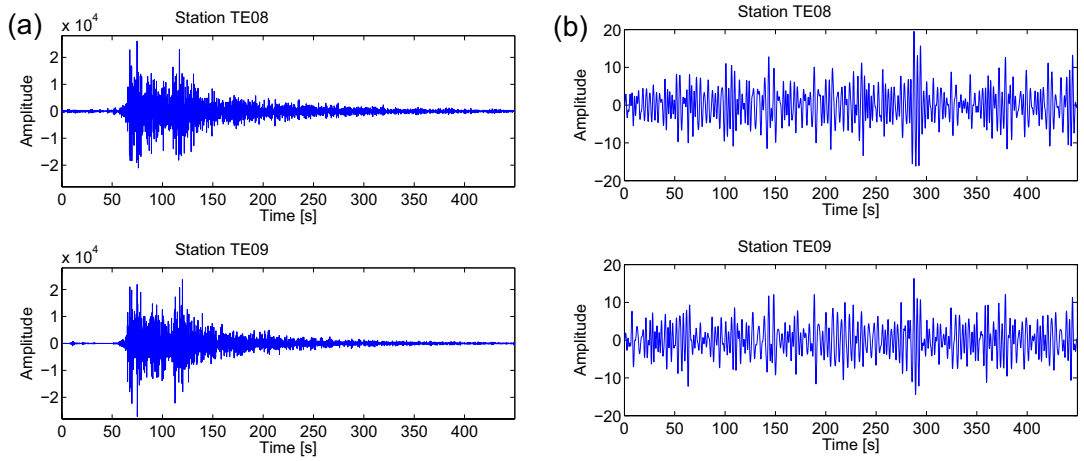

Fig. 6. Examples of recordings of vertical ground velocity, detected at station TE08 (top) and TE09 (bottom). (a) A response of a regional earthquake. (b) A microseism response.

The T-array was installed partly in January and partly during the second field campaign in March-April. Figure 5(b) shows an example station. The stations from this array consist of the same equipment as the ones in the P-array.

For both arrays we use L-22 sensors, which have a corner frequency of 2 Hz. Although these sensors are designed for recording frequencies above 2 Hz, still accurate amplitudes are obtained down to 0.1 Hz, given that the data is corrected for the instrument response [31]. The instrument response shows variability from sensor to sensor below the corner frequency. Therefore, we measured the instrument response of each sensor, just after installation. Additionally, at the middle station of the TN-subarray (fig. 2) we installed both a short-period sensor (L-22) and an intermediate-period sensor (CMG 40T) with a corner frequency of 0.033 Hz. The L-22 response will be compared with the broadband reference sensor. Hence, we can assess until what extent frequencies below 0.1 Hz can still be used for qualitative purposes.

Figure 6(a) shows an example of earthquake records, as detected with two stations of the TE subarray. These regional earthquakes are detected a few times per day. Figure 6(b) shows an example of microseism recordings. Microseisms are recorded continuously and are related to ocean-wave interactions. Both the earthquake and the microseism records are used for source location and inferring information of the Earth's properties between the two stations.

5 Future plans

The seismic stations that were installed in 2012 in the Malargüe region are meant as a temporary array, whose data will serve as a preliminary study for the installation of a permanent array in the region. In 2015, the complete data will become publicly available through IRIS.

The data recorded by the temporary array are being stored locally at each station. The recorded data is collected from the stations of the T-array approximately every 3 months, while from the P-array it is collected with the same frequency only outside the winter months. During the winter, the Peteroa area is covered by heavy snow, which precludes access to the P-array. For this, the data is being recorded and stored locally at stations during the complete winter (approximately from mid-April till mid-October). To avoid such delays in data availability, for the permanent array we want to make use of instantaneous data transfer using telemetry. This will also be useful for hazard assessment purposes.

When a sufficient quantity of data is collected from the stations, the implementation of the above-explained techniques will be started. Depending on the results, we will decide what the geometry of the future permanent array would be and what instruments would be best to use.

We are also investigating the possibility to install, as part of the permanent array, deformation sensors. These will be used to monitor surface deformation, for example due to expansion or contraction of Peteroa's magma chamber. Together with the seismic array, this would allow for even better understanding of the volcanic processes.

We are also aiming at a collaboration with PA projects for the research benefits of both sides. Reference [32] describes the large collection of atmospheric measurements and cosmic-ray detectors installed in the Malargüe region. The unique collocation of all these measuring devices together with a seismic array, allows to study the coupling of cosmic, atmospheric and seismic signals. For example, the coupling from lightning (and thunder) to Earth vibration

can be accurately studied, using the fluorescence and surface detectors [32] and the lightning-mapping array [33] for timing, location and intensity of the lightning, and the seismic stations for characterizing the induced ground vibration.

Reference [34] reported that a decrease in the PA (cosmic) particle-detection rate (see also [32]) was observed just after the 8.8 Central Chile (Maule) earthquake from February 27, 2010. The author reported that the timing of the decrease roughly coincides with the estimated arrival of S-waves from the earthquake at the PA surface detectors. The author reported that during the six years of operation of the stations no other such phenomenon has been detected, even though small earthquakes have occurred. Reference [35] investigated the influence of the 9.0 Tohoku-Oki earthquake from March 11, 2011 on the ionospheric total electron content observed by GPS satellites. The author reported ionospheric disturbances following just after the earthquake, inferred from GPS data. The ionospheric changes could be caused by earthquake-induced atmospheric waves. Moreover, the author reported precursory changes in the total electron content starting about 40 minutes before the earthquake. The author investigated also the effect of the Chilean earthquake on the total electron content in the ionosphere and found the same precursory change. The earthquake was followed by coseismic disturbances as well. The inferred changes in the ionosphere reported by [35] are not necessarily related to the particle-detection rate observed in the troposphere as reported in [34]. Both references show a drop in inferred particle changes occurring not until after the earthquake.

At this point, it is unknown whether the detection-rate change at the PA stations, due to the 2010 Maule earthquake was caused by an instrumental effect or an actual change in the particle flux. A permanent seismic array that is partly collocated with stations from the PA Observatory would allow for a better analysis of the effect of earthquakes on the measured particle-detection rate. Using the recordings from the individual stations, a drop in particle-detection rate can much better be linked to specific seismic-wave arrivals. The further addition of a few infrasound stations would allow studying the coupling from seismic to atmospheric waves and the possible link between atmospheric waves and charged particles in the atmosphere. The amplitude of the detected seismic waves is a function of the local soil conditions. If the change in particle-detection rate is an instrumental effect, PA stations that are on softer soil and therefore endure larger vibrations, likely would show a larger coseismic anomaly. On the other hand, if severe earthquakes do in fact lead to charged-particle changes in the atmosphere, the PA anomaly is expected to show little spatial variation over the PA array. Besides the major earthquakes, the seismic array detects and locates abundant regional seismicity. This allows studying the presumed seismic sensitivity of the PA detectors over a broad range of earthquake distances, depths and magnitudes.

We thank the Argentine Ministry of Science and Education for the partial financial support. We thank IRIS-PASSCAL for providing the seismic equipment. We thank the Juan Agulles, Mayer of Malargüe, the department of Civil Defense of Malargüe and the gendarmerie personnel at Peteroa for their continuous help before, during and after the installation of the seismic stations. We thank Pierre Auger for the help during the installation. The research of ER is sponsored by ISES (The Netherlands Research Centre for Integrated Solid Earth Sciences). We thank Lawrence Wiencke for helpful suggestions.

References

1. O. Yilmaz, S.M. Doherty, *Seismic data analysis: processing, inversion and interpretation of seismic data* (SEG, 2000).
2. J. Rickett, J.F. Claerbout, The Leading Edge **18**, 957 (1999).
3. G.T. Schuster, J. Yu, J. Rickett, Geophys. J. Int. **157**, 838 (2004).
4. K. Wapenaar, Geophysics **68**, 1756 (2003).
5. A. Bakulin, R. Calvert, Geophysics **71**, SI139 (2006).
6. D. Draganov, K. Wapenaar, W. Mulder, J. Singer, A. Verdel, Geophys. Res. Lett. **34**, L04305 (2007) doi:10.1029/2006GL028735.
7. E.N. Ruigrok, X. Campman, K. Wapenaar, C. R. Geosc. **343**, 512 (2011).
8. S. Abe, E. Kurashimo, H. Sato, N. Hirata, T. Iwasaki, T. Kawanaka, Geophys. Res. Lett. **34**, L19305 (2007) doi:10.1029/2007GL030633.
9. D. Draganov, X. Campman, J. Thorbecke, A. Verdel, K. Wapenaar, Geophysics **74**, A63 (2009).
10. E.N. Ruigrok, X. Campman, D. Draganov, K. Wapenaar, Geophys. J. Int. **183**, 339 (2010).
11. L. Knopoff, Geophys. J. Int. **4**, 161 (1961).
12. M.S. Longuet-Higgins, Philos. Trans. R. Soc. London, Ser. A **243**, 1 (1950).
13. N.M. Shapiro, M. Campillo, Geophys. Res. Lett. **31**, L07614 (2004) doi:10.1029/2004GL019491.
14. H. Yao, R.D. van der Hilst, M.V. de Hoop, Geophys. J. Int. **166**, 732 (2006).
15. C.A. Langston, J. Geophys. Res. **84**, 4749 (1979).
16. K. Wapenaar, J. van der Neut, E.N. Ruigrok, Geophysics **75**, A51 (2008).
17. K. Wapenaar, E. Ruigrok, J. van der Neut, D. Draganov, Geophys. Res. Lett. **38**, L01313 (2011) doi:10.1029/2010GL045523.
18. S. Rost, C. Thomas, Rev. Geophys. **40**, 1008 (2002) doi:10.1029/2000RG000100.
19. K.D. Koper, K. Seats, H. Benz, Bull. Seismol. Soc. Am. **100**, 606 (2010).
20. P. Diodati, P. Bak, F. Marchesoni, Earth Planet. Sci. Lett. **182**, 253 (2000).

21. R. Snieder, A. Grêt, H. Douma, J. Scales, Science **295**, 2253 (2002).
22. M.M. Haney, K. van Wijk, L.A. Preston, D.F. Aldridge, Lead. Edge **28**, 554 (2009).
23. C. Sens-Schönfelder, U. Wegler, Geophys. Res. Lett. **33**, L21302 (2006) doi:10.1029/2006GL027797.
24. N.M. Shapiro, M. Campillo, L. Stehly, M.H. Ritzwoller, Science **307**, 1615 (2005).
25. F. Brenguier, N.M. Shapiro, M. Campillo, A. Nercessian, V. Ferrazzini, Geophys. Res. Lett. **34**, L02305 (2007) doi:10.1029/2006GL028586.
26. M.R. Daneshvar, C.S. Clay, M.K. Savage, Geophysics **60**, 1178 (1995).
27. M. Landes, F. Hubans, N.M. Shapiro, A. Paul, M. Campillo, J. Geophys. Res. **115**, B05302 (2010).
28. R.L. Nowack, S. Dasgupta, G.T Schuster, J.-M. Sheng, Bull. Seismol. Soc. Am. **96**, 1 (2006).
29. E. Ruigrok, K. Wapenaar, Geophys. Res. Lett. **39**, L11303 (2012) doi:10.1029/2012GL051672.
30. I. Panea, D. Draganov, C. Almagro Vidal, V. Mocanu, unpublished.
31. E Arias, N. Barstow, unpublished.
32. L. Wiencke, Eur. Phys. J. Plus **127**, 98 (2012).
33. W.C. Brown, J.R. Dywer, P.R. Krehbiel, W. Rison, R.J. Thomas, H. Edens, Eur. Phys. J. Plus **127**, 95 (2012).
34. H. Asorey, 2011, *Proceedings of the 32nd International Cosmic Ray Conference* (Beijing).
35. K. Heki, Geophys. Res. Lett. **38**, L17312 (2011) doi:10.1029/2011GL047908.